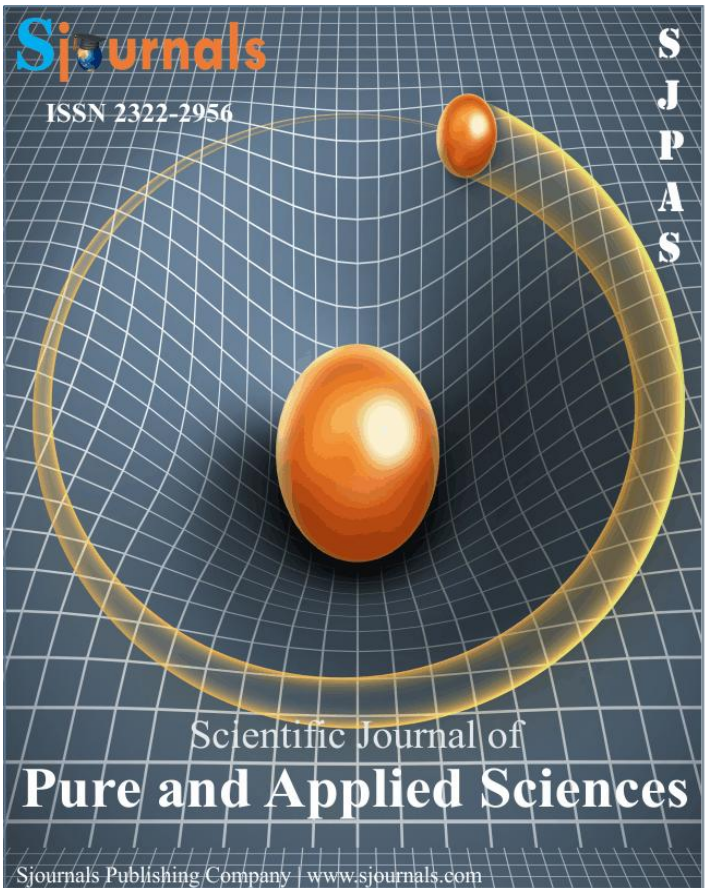

Scientific Journal of Pure and Applied Sciences (2017) 6(9) 635-650
ISSN 2322-2956
doi: 10.14196/sjpas.v6i9.2430

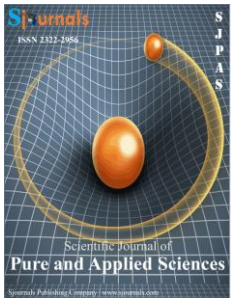

Contents lists available at Sjournals
Scientific Journal of **Pure and Appiled Sciences**
Journal homepage: www.Sjournals.com

Original article

Experimental and numerical studies of laminated butt joint specimens with Aluminum butt straps under preload

Sringeri Srikanta Subramanya Sastry[a,*], Venkata Siva Nagaraju Reddy[b], Kasi Ramjeyathilagam[c]
[a]*Research Scholar, Hindustan University, School of Aeronautical Sciences, Chennai 603103, India.*
[b]*M. Tech Student, JNTU Kakinada, Andhra Pradesh 533 033, India.*
[c]*Senior Professor, Hindustan University, School of Aeronautical Sciences, Chennai 603103, India.*

*Corresponding author: ss.subramanyasastry@cyient.com

ARTICLE INFO

Article history,
Received 17 August 2017
Accepted 03 September 2017
Available online 10 September 2017
iThenticate screening 19 August 2017
English editing 01 September 2017
Quality control 08 September 2017

Keywords,
Butt joint
Butt straps
Matched die moulding
Characteristic curve
Bearing failure boundary
Least square method

ABSTRACT

Experimental and numerical investigations on laminated butt joint specimens (size 72 mm x 135 mm x 3.328 / 4.502 / 5.672 mm thickness) with Aluminium butt straps under preload are presented. Five specimens each of three different thickness using 6781 8HS S2 glass fabric with quasi-isotropic layup were fabricated, assembled and tested to study their failure behavior. The specimens with two bolts in parallel and series were designed to twice the width mentioned in ASTM D 5961/D 5961M – 08, fabricated by matched die moulding process for the study of bearing strength and ultimate load carrying capacity of a eight bolted butt joint. The width of the specimens, edge distance and pitch of the M6 fasteners were adjusted so as to be within the limits of the Instron testing machine with Zwick-Roell grips. The experimental results were compared with the numerical results of a 3D finite element model developed from a Catia model that incorporates a characteristic curve around the bolt holes of the butt joint. The points on the bearing failure boundary around each fastener hole was compared with the curve approximated using the least square method. It was observed that the theoretical characteristic curve has shown deviation to the curve fitted using least square method on the experimental data.

1. Introduction

Failure of bolted joints in laminated composites load carrying members is a very important topic in various aircraft structures. It is important to understand the various types of failure modes in such structures in order to design an efficient joint against various modes of failure. Understanding the various types of failures has still remained as a challenge to the designer. Thus, there is a continuous need to understand the behaviour of bolted joints subjected to various types of loads for assessing the vulnerability of the joint to failure and efficiently design the joint against such failures. The analysis involving bolted joints is complex due to the various issues involved like effects of friction, clearance or interference, effect of preload, contact areas, change of failure modes from one type to another to name a few. Camanho and Matthews (1997) have presented a detailed review of stress analysis and strength prediction of mechanically fastened joints and established five common modes of failure in mechanically fastened joints in composites namely, net tension, shear, bearing, cleavage and pull through.

Effects of friction on bolted and pinned composite joints were studied in detail experimentally and numerically by McCarthy and other researchers on these failure modes (Shirazi and Zareb, 2013; Nasraoui et al., 2013; Ivana et al., 2011; Gray and McCarthy, 2010; Katsumata et al., 2010; McCarthy et al., 2005; Xiao et al., 2000) and they established that the inclusion of friction can provide useful insight for the design of composite joints. Effect of clearance between the bolt hole and the bolt studied in detail by McCarthy et al. (2002) indicated that increase in clearance resulted in reduced joint stiffness and increased ultimate strain (McCarthy and McCarthy, 2013; McCarthy and McCarthy, 2005; McCarthy et al., 2002). The effect of bolt layout on the mechanical behavior of the joints studied using 3D finite element analysis and simplified analytical methods by Khurshid (2013), Yang et al. (1998) has shown good agreement of results between the predicted and experimental results (Sen et al., 2007). The composite joints are analyzed using alternate methods like the X-ray diffraction (XRD) techniques, 3D finite element analysis to assess the effect of various parameters (Camanho and Matthews, 1997; Sreeshankar et al., 2014; McCarthy et al., 2005). Using simplified and rigorous mathematical methods the composite joints analyzed by authors like Yang et al. (1998) and Binqi et al. (2015) these have shown good agreement between the experimental results. Effect of preload was studied in detail by Kunliang et al. (2013), Abid and Mehmood Khan (2013), Sen et al. (2007). The effect of contact was considered in all the above studies while predicting the strength of the composite bolted joints (Camanho and Matthews, 1997; Hilton, 2016).

In the present study, experimental and numerical investigations on laminated butt joint specimens (size 72 mm * 135 mm * 3.328 / 4.502 / 5.672 mm thickness) with laminated butt straps under preload are presented. Five specimens each of three different thickness using 6781 8HS S2 glass fabric with quasi-isotropic layup; were fabricated, assembled and tested to study their failure behavior. The specimens with two bolts in parallel and series were designed to twice the width mentioned in ASTM D 5961/D 5961M – 08, fabricated by matched die moulding process for the study of bearing strength and ultimate load carrying capacity of a eight bolted butt joint. The experimental results were compared with the numerical results of a 3D finite element model developed from a Catia model that incorporates a characteristic curve around the bolt holes of the butt joint. The points on the bearing failure boundary around each fastener hole was compared with the curve approximated using the least square method.

2. Problem statement

Detailed experimental and numerical investigation of a laminated butt joint specimen consisting of two quasi-isotropic laminates with two Aluminum butt straps (AA6061-T4) connected through 8 bolts (Fig. 1) under tensile load were carried out. The specimens with two bolts in parallel and series were designed to twice the width mentioned in ASTM D 5961/D 5961M – 08, fabricated by matched die moulding process for the study of ultimate load carrying capacity of a eight bolted butt joint. The width of the specimens, edge distance and pitch of the M6 fasteners were adjusted so as to be within the limits of the Instron testing machine with Zwick-Roell grips.

3. Geometry and fabrication of test specimens

The test specimen is an assembly of two laminates 72 mm * 135 mm, two Aluminum alloy (AA6061-T4) butt straps 72 mm * 135 mm (Fig. 1). The two laminates with a gap of 1 mm between them with two 5 mm thick butt straps were assembled as shown in Fig. 1. Three types of test specimens are fabricated using laminates of 3, 4 and

5 mm thickness (5 specimens for each thickness and total of 15 specimens). These laminates as fastened together using Unbrako M6 bolts (6.0 mm average diameter, Fig. 2) with two 1 mm thick steel washers one on the head and nut side (Fig. 2). The laminates are fabricated using 6781 S2 glass fabric of 8HS weave (58 yarns / inch in warp and 54 yarns / inch in fill directions) with an areal density of 297 gm / sq.m. The achieved average ply and specimen thickness is shown in Table 1 and assembled test specimen is shown in Fig. 3.

Table 1
Achieved specimen and average ply thickness per actual measurement.

Sl. No.		**Measured thickness**		
Specified thickness (3 mm)	**Specimen No.**	**Left (mm)**	**Right (mm)**	**Average ply thickness (mm)**
1	T3D6E3D6-1*	3.36	3.34	3.328
2	T3D6E3D6-2	3.28	3.32	
3	T3D6E3D6-3	3.38	3.48	
4	T3D6E3D6-4	3.28	3.28	
5	T3D6E3D6-5	3.34	3.28	
Specified thickness (4 mm)				
1	T4D6E3D6-1	4.52	4.48	4.502
2	T4D6E3D6-2	4.48	4.50	
3	T4D6E3D6-3	4.52	4.52	
4	T4D6E3D6-4	4.48	4.48	
5	T4D6E3D6-5	4.52	4.50	
Specified thickness (5 mm)				
1	T5D6E3D6-1	5.60	5.70	5.672
2	T5D6E3D6-2	5.64	5.62	
3	T5D6E3D6-3	5.72	5.74	
4	T5D6E3D6-4	5.74	5.72	
5	T5D6E3D6-5	5.62	5.62	

* Specimen Nomenclature: T3 - Specimen thickness is 3 mm, D6 - Diameter of bolt is 6 mm, E3 - Edge distance is 3*Diameter of bolt, D6 - Pitch of the bolts is 6*Diameter of the bolt.

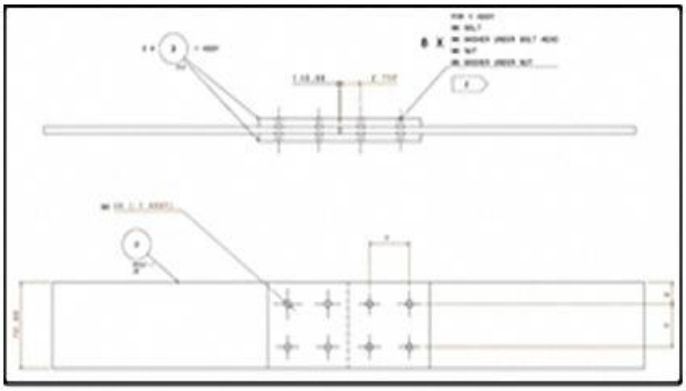

Fig. 1. Geometry of the assembled test specimen.

Fig. 2. Unbrako high strength steel fastener.

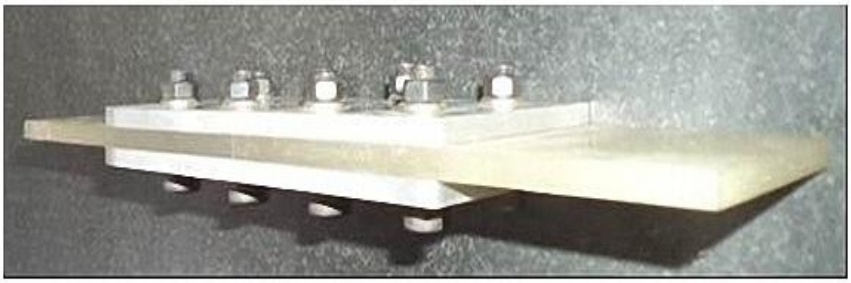

Fig. 3. Assembled test specimen.

3.1. Preparation of test specimens

3.1.1. Mould preparation

The specimens required for the testing are cut from laminates 3 mm, 4 mm and 5 mm thickness. The moulds used for preparing laminates were prepared out of 30 mm thick EN 8 steel plate. The mould consists of a pair of male and female moulds. The outer dimensions of the female mould were 500 * 400 * 30 mm. A cavity measuring 402 * 302 * 10 mm was scooped out by CNC milling operation, leaving a clear border of 98 mm around the mould. The male mould consists of EN 8 steel plate of 30 mm thick, on which additional plates of 7 mm, 6 mm and 5mm can be fitted based on the thickness of laminate to be produced by proper bolts leaving a clear border of 100 mm around the attached plates. When the top and bottom moulds are closed, by attaching additional plate to the top mould based on the required thickness of laminate 3 mm, 4 mm and 5 mm can be formed between the two matched moulds (Fig. 4). The surface of the moulds is treated with protective layer of chrome plating of 50 micron thick.

Fig. 4. Matched die mould of EN 8 steel plate.

The surface of the moulds are prepared using releasing coat (Safelease 30) before the layup to ensure the release of laminate from the mould after curing. LY556 resin, HY905 hardener, DY040 plasticizer and DY062 accelerator are mixed in the ratio of 100:100:10:0.02 with the help of stirrer. 6781 8HS S2 glass prepreg was manufactured by using predetermined quantity of S2 glass fabric and resin mix, by coating the mixed resin on to the 6781 8HS S2 glass fabric. A template of size 400 mm * 300 mm was prepared from Mylar film. Predetermined number of prepreg layers are cut as per layup orientation and placed into the mould cavity as per the sequence given in Table 2 to build up the required thickness of the laminates. The number of layers required to build 3 mm, 4 mm and 5 mm laminates are 14, 18 and 22. Then male mould is attached with required additional plate of thickness (7mm, 6mm and 5mm thickness). The top and bottom moulds are secured on to each other by fixing nut-bolt and ensure the closing of moulds is without gaps.

3.1.2. Curing

Mould in the closed condition is transferred to the appropriate heating oven to carry out the polymerization by using the following curing cycle.

- Raise the temperature from ambient to 90^{o}C @ the rate of 1^{o}C/minute
- Hold the temperature at 90^{o}C for 60 minutes
- Raise the temperature from 90 to120^{o}C @ the rate of 1^{o}C/minute
- Hold the temperature at 120^{o}C for 60 minutes
- Raise the temperature from 120 to 165^{o}C @ the rate of 1^{o}/minute
- Hold the temperature at 165^{o}C for 60 minutes
- Then the laminates are cured to room temperature

The cured laminates are tested for fiber volume fraction and the results are presented in Table 3.

3.1.3. Specimen preparation

The required sizes of specimens are cut from the laminate of specified thickness and subjected to the finishing process. Since these specimens don't require any end tabs (ASTM D 5961 / D 5961M-08, 2010), no

provision for tabs is provided. However, both ends of the specimens are roughened by diamond shaped scratches to facilitate proper gripping in the end grips of the Instron testing machine.

Table 2
Ply sequence for three laminates.

Sl. No.	No. of plies	Ply sequence	D (mm)	(E/D)	(W/D)	Pitch (mm)
1	14	$(0/45/90/-45/0/45/90)_{SYM}$	6	3	12	6D
2	18	$(0/45/90/-45/0/45/90/-45/0)_{SYM}$	6	3	12	6D
3	22	$(0/45/90/-45/0/45/90/-45/0/45/90)_{SYM}$	6	3	12	6D

Table 3
Fiber volume fraction of the cured laminates.

Charging temp. (^oC)	Soaking temp. (^oC)	Thickness (mm)	Duration (Hrs)	Percentage of resin	Percentage density of glass (gm/cc)
345	565 ± 20	3.328	436.61	63.43	1.75
345	565 ± 20	4.502	436.22	63.77	1.71

3.1.4. Assembly

Specimen is assembled with the help of two FRP plates of same sizes and two Aluminum butt straps. Drilling of 8 holes onto the specimen assembly is carried out with the help of jig and fastening is carried out as shown in Fig. 3. M6 Unbrako bolts were tightened to a torque of 2.2 N-m (ASTM D 5961 / D 5961M-08, 2010).

4. Experiments

Testing of specimens were conducted in the Instron testing machine (Fig. 5, Advanced Composites Division, NAL, Bangalore) with Zwick-Roell grips at a cross head speed of 2 mm / minute as per ASTM D 5961/D 5961M-08 per Procedure A (bolts under double shear, tension). The specimens are scratched lightly so as not to disturb the layers, but to provide serrated surface of 72 mm * 25 mm area at the two ends of the laminates for better gripping between the upper and lower jaws of the Instron testing machine as shown in Fig. 6. During the testing process load versus cross head displacement curves were plotted via the computer that was controlling the experimentation process. Each set comprising of 5 specimens numbered as shown in Table 1 is loaded up to failure; load and cross head displacements were recorded. The specimens failed at two different locations along the line joining bolts 1 & 2 and 5 & 6. During the course of the experiment, bearing failure was observed at all bolt locations followed by the net tension failure mode. The photographs of the failed specimens is presented in Fig. 7 and Fig. 8 (specimens of thickness 3.328 mm), Fig. 9 (AA6061-T4 butt strap, 5 mm thickness and Fig. 10 and 11 (specimens of thickness 4.502 mm and 5.672 mm). The failure of specimens observed is shown in Table 4.

Fig. 5. Test set up on Instron universal testing machine.

Table 4
Observed failure sections in specimens.

Specimen	Section of failure	Side (Right / Left)	Location Grip / Load
T3D6E3W6-1	Line joining Bolt 1 – Bolt 2	Right	Grip
T3D6E3W6-2	Line joining Bolt 1 – Bolt 2	Right	Grip
T3D6E3W6-3	Line joining Bolt 1 – Bolt 2	Right	Grip
T3D6E3W6-4	Line joining Bolt 5 – Bolt 6	Left	Load
T3D6E3W6-5	Line joining Bolt 5 – Bolt 6	Left	Load
T4D6E3W6-1	Line joining Bolt 1 – Bolt 2	Right	Grip
T4D6E3W6-2	Line joining Bolt 1 – Bolt 2	Right	Grip
T4D6E3W6-3	Line joining Bolt 5 – Bolt 6	Left	Load
T4D6E3W6-4	Line joining Bolt 5 – Bolt 6	Left	Load
T4D6E3W6-5	Line joining Bolt 5 – Bolt 6	Left	Load
T5D6E3W6-1	Line joining Bolt 1 – Bolt 2	Right	Grip
T5D6E3W6-2	Line joining Bolt 1 – Bolt 2	Right	Grip
T5D6E3W6-3	Line joining Bolt 5 – Bolt 6	Left	Load
T5D6E3W6-4	Line joining Bolt 1 – Bolt 2	Right	Grip
T5D6E3W6-5	Line joining Bolt 5 – Bolt 6	Left	Load

Fig. 6. Roughened end strips of specimen.

Fig. 7. Failure mode in experiment for T3D6E3W6-1.

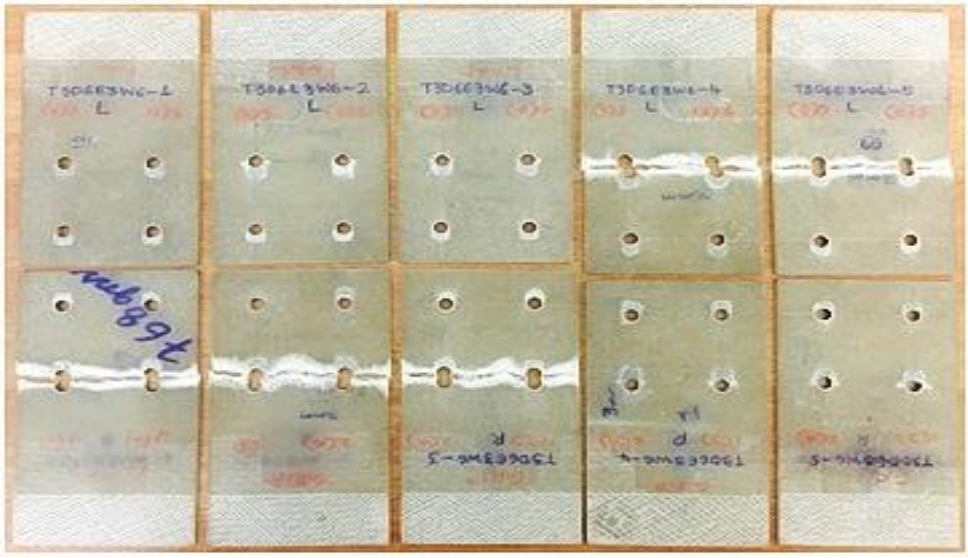

Fig. 8. Failed specimens of thickness 3.328 mm.

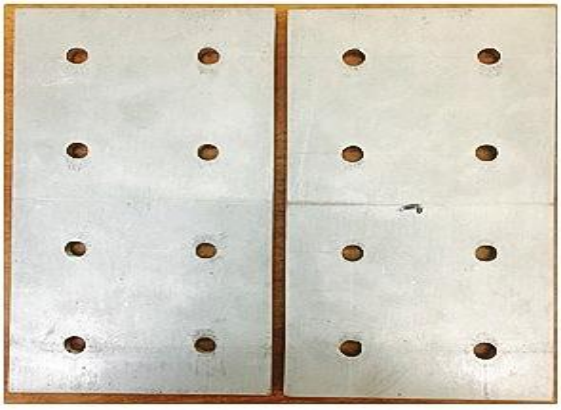

Fig. 9. View of Aluminum butt straps.

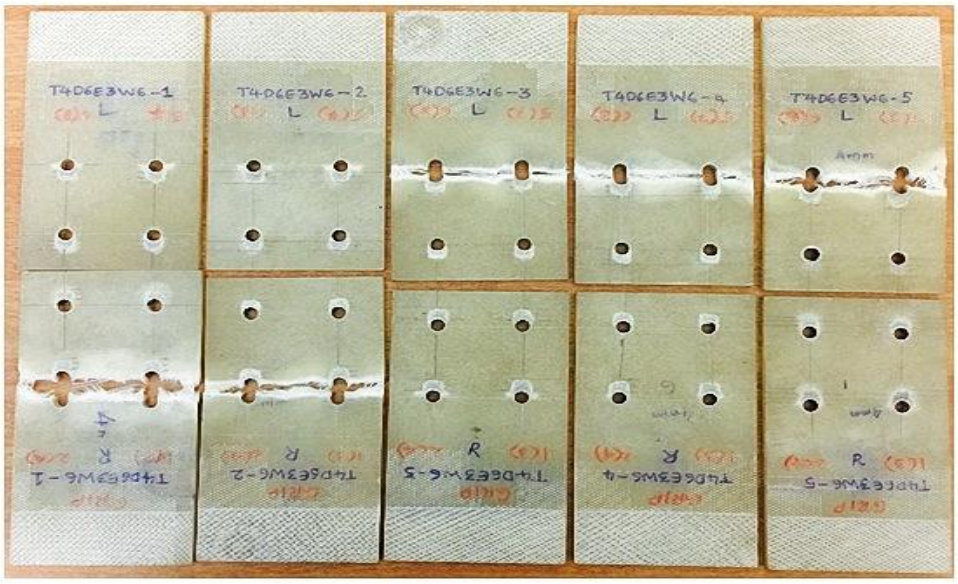

Fig. 10. View of failed specimens of thickness 4.502 mm.

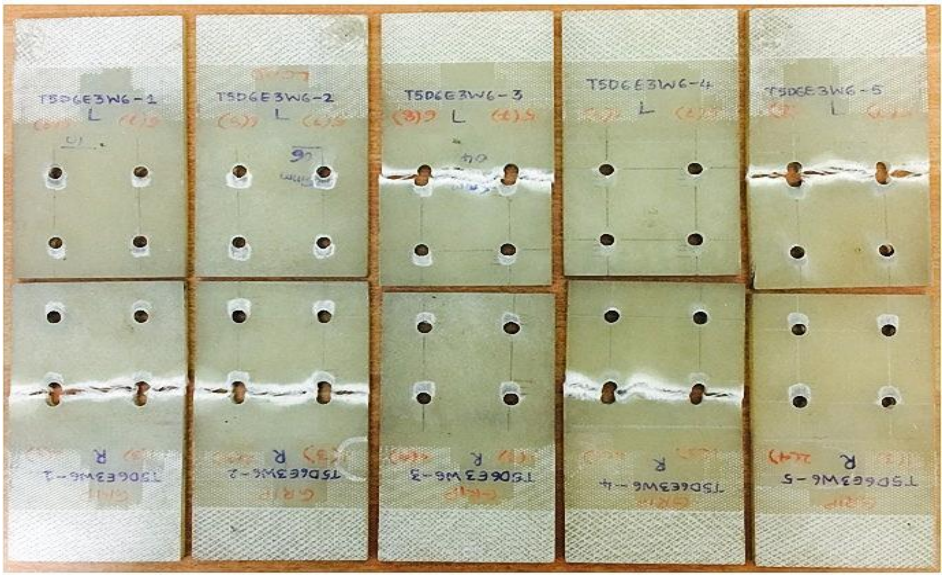

Fig. 11. View of failed specimens of thickness 5.672 mm.

5. Numerical study

To investigate the joint behavior, three dimensional finite element models with quasi-isotropic laminate properties (ASTM D 5961 / D 5961M-08, 2010) were created using the SOLID185–3-D 8-Node Solid element available in ANSYS mechanical finite element software. The GFRP laminate, butt straps, bolts and washers were modeled using SOLID185 having three displacement degrees per node. Surface to surface contact between the bolt shank and the bolt hole inner surface was defined using the CONTA174 (bolt) and TARGE170 (laminate) elements. Bolt preload was simulated using PRETN179 elements. Coulomb friction model was used to introduce friction between the shank of the bolt and the laminate surface inside the bolt hole. Clamped end conditions are simulated at one end and the load is applied on the other end of the model (Fig. 12). As a special feature of these finite element models, a characteristic curve was introduced into the model. This model will help in understanding the bearing mode of failure around the bolt holes as per the suggestion by Ivana et al. (2011). The details of the characteristic dimensions used for this curve is shown in Table 5. Geometric nonlinear analysis is conducted with contact between the shank of the bolts and the laminate at all eight locations with friction coefficients (0.05, 0.1, 0.15 and 0.8). The displacements of the models were compared between the experiments and finite element models and are shown in Table 6.

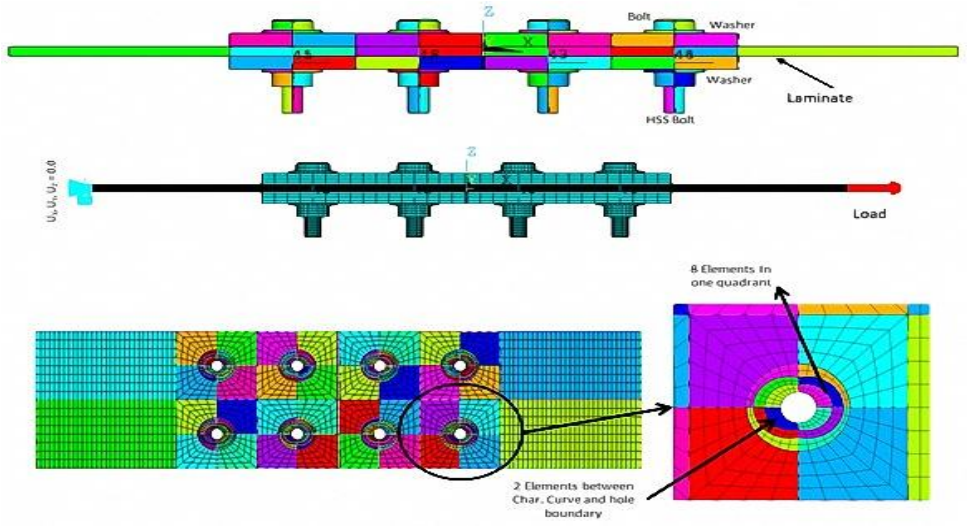

Fig. 12. Finite element model of the specimen.

Table 5
Parameters of the embedded characteristic curve in the finite element model.

Sl. No.	Description	Value (mm)
1	Diameter of the hole	6.0
2	Characteristic Length in tension, R_{ot}	1.17
3	Characteristic Length in compression, R_{oc}	2.4

Table 6
Comparison of hole and specimen deformations.

Sl. No.	Description	Test results	FEA results (mm)	Percentage difference w.r.t. test
1	Hole Deformation T3D6E3W6-1 to 3	1.67	1.65	1.20
2	Hole Deformation T3D6E3W6- 4 & 5	1.75	1.65	5.71
3	Hole Deformation T4D6E3W6-1 & 2	2.00	1.71	14.50
4	Hole Deformation T4D6E3W6- 3 to 5	1.83	1.71	6.56
5	Hole Deformation T5D6E3W6-1 to 3	2.67	1.83	31.46
6	Hole Deformation T5D6E3W6- 4 & 5	3.00	1.83	39.00
7	Specimen Deformation T3D6E3W6-1 to 3	3.00	2.65	11.67
8	Specimen Deformation T3D6E3W6- 4 & 5	2.75	2.65	3.64
9	Specimen Deformation T4D6E3W6-1 & 2	2.75	2.71	1.45
10	Specimen Deformation T4D6E3W6- 3 to 5	4.17	2.71	35.01
11	Specimen Deformation T5D6E3W6-1 to 3	3.67	2.88	21.52
12	Specimen Deformation T5D6E3W6- 4 & 5	4.00	2.88	28.00

5.1. Material model

The elastic and strength properties of bidirectional 6781 8HS S2 glass cloth (Michelle, 2013), AA6061-T4 (MMPDS-07, 2012) butt strap and Unbrako bolt high strength steel (Unbrako Engineering Guide) used in the analysis are given in Table 7, 8 and 9.

Table 7
Properties of the lamina.

Sl. No.	Property	Value
1	Young's Modulus (E_1, MPa)	29095.88
2	Young's Modulus (E_2, MPa)	27889.29
3	Young's Modulus (E_3, MPa)	27889.29
4	Shear Modulus (G_{12}, MPa)	3792.12
5	Shear Modulus (G_{23}, MPa)	379.12
6	Shear Modulus (G_{31}, MPa)	379.12
7	Poisson's Ratio (μ_{12})	0.14
8	Poisson's Ratio (μ_{23})	0.14
9	Poisson's Ratio (μ_{31})	0.14
10	Fiber strength (longitudinal, X_t, MPa)	551.58
11	Fiber strength (longitudinal, X_c, MPa)	558.47
12	Fiber strength (Transverse, Y_t, MPa)	544.68
13	Fiber strength (Transverse, Y_c, MPa)	461.94
14	Fiber strength (In plane, S_{12}, MPa)	63.15
15	Fiber strength (Out of plane, S_{23}, MPa)	174.05[#]
16	Fiber strength (Out of plane, S_{31}, MPa)	63.15

calculated as per recommendations of Libin et al., (2015).

Table 8
Properties of the AA6061-T4 butt straps.

Sl. No.	Property	Value
1	Young's Modulus (E, MPa)	68258.11
2	Poisson's Ratio (μ_{12})	0.33

Table 9
Properties of the Unbrako high strength steel bolt.

Sl. No.	Property	Value
1	Young's Modulus (E, MPa)	210000
2	Poisson's Ratio (μ_{12})	0.31

6. Results and discussion

6.1. Experimental results

During this experimental study, three groups of composite laminate specimens of 5 specimens each were tested. Every specimen was loaded up to failure of the specimen. For each specimen, a load versus cross head displacement curves was obtained as shown in Fig. 13, 14 and 15. Earlier studies conducted by Sen et al. (2007) had used specimens with 0^0 and 45^0 plies in the laminates, whereas, in this study (0/45/90/45) layup is used to build the required thickness as recommended by ASTM D 5961 / D 5961M-08 (2010). They concluded that as the E/D ratio is greater than 2 (in the present cases, it is 3) mixed or bearing failure mode develops which is the best mode of failure for resisting tensile load. In the present study, it is observed that no specimens have shown cleavage and shear out modes of failure because the specimens were designed as per the recommendations of ASTM D 5961 / D 5961M-08 (2010). In this study, each specimen has shown bearing failure at each bolt location followed by a net section failure at ultimate load.

The load-cross head displacement curve is nonlinear till ultimate failure load. In the initial stage of loading, the load is first picked up by the matrix and then subsequently by fibers. In this stage the elongation of the matrix is more when compared to the elongation of the fiber. As the load increases, the matrix transfers all the load to the fibers. At this stage major portion the load is carried by the fiber while a small portion is carried by matrix surrounding the fiber. As the load further increases, the fibers start breaking and lose the load carrying capacity rapidly. At this stage, the load is fully transferred to the surrounding matrix. The strain caused by this high load is above the strain sustainable by the matrix. Simultaneously, at this point the matrix also yields and the specimen breaks. This is indicated by the quick decrease in the load carried by the specimen. At this stage, the specimen is completely broken and the load drops off.

From the Fig. 13, it is observed that for the specimens T3D6E3W6-1, T3D6E3W6-2, T3D6E3W6-3 and T3D6E3W6-5 failure has occurred when crosshead displacement was in the range of 8 to 9 mm. But for the specimen T3D6E3W6-4 the failure has occurred when crosshead displacement was close to 10 mm. From Fig. 14, it is observed that for the specimens T4D6E3W6-1, T3D6E3W6-2, T3D6E3W6-4 and T3D6E3W6-5 specimens the failure has occurred when crosshead displacement was in the range of 9 to 11 mm. For T4D6E3W6-3 the failure has occurred when the cross head displacement is between 11 to 12 mm. T4D6E3W6-5 has shown more elongation than other specimens. From Fig. 15 it is observed that for the specimens T5D6E3W6-4 and T3D6E3W6-5 the failure has occurred when crosshead displacement was in the range of 10 to 11 mm. It is also observed that the range of crosshead displacement is more (8 to 11 mm approximately) for specimens of lower thickness (3.328 mm) whereas it is less (9.5 to 11 mm approximately) for specimens of higher thickness (4.504 and 5.664 mm). From this it is concluded that specimens of lowest thickness have more flexibility than the specimens of higher thickness.

From Tables 10, 11 and 12 it is observed that the coefficient of variation of T4D6E3W6 specimens is the least (2.42%) followed by T3D6E3W6 (3.36%) and T5D6E3W6 (3.66%). This indicates that the 4.504 mm laminate has shown more uniform structural behavior as compared to other two laminates (3.328 and 5.665 mm thick) followed by 3.328 mm thick laminate and 5.665 mm thick laminates from which the specimens are prepared. Similar observation applies for standard deviation also.

All the specimens were gripped between the upper and lower loading grips (Fig. 5). The lower grip is stationary and the load is applied by the movable upper grip. From Table 4, it is observed that for specimens T3D6E3W6-1, T3D6E3W6-2, T3D6E3W6-3 net tension failure at ultimate load occurred along the line joining the bolts 1 and 2 on the right hand side close to the moving upper grip. The failure of the specimen (T3D6E3W6-1) at ultimate load was clearly seen in Fig. 5. Similarly, for specimens T3D6E3W6-4 and T3D6E3W6-5 the failure was observed on the lower loading grip which was stationary along the line joining bolts 5 and 6. For specimens T4D6E3W6-1 and T4D6E3W6-2 net tension failure at ultimate load occurred along the line joining the bolts 1 and 2 on the right hand side close to the moving upper grip. Similarly, for specimens T4D6E3W6-3, T4D6E3W6-4 and T4D6E3W6-5 the failure was observed on the lower stationary grip along the line joining bolts 5 and 6. But in specimens with 5.664 mm thick, it was observed that the specimens T5D6E3W6-1, T5D6E3W6-2 and T5D6E3W6-4 net tension failure at ultimate load occurred along the line joining the bolts 1 and 2 on the right hand side close to the moving upper grip. Similarly, for specimens T5D6E3W6-3 and T5D6E3W6-5 the failure was observed on the lower stationary grip along the line joining bolts 5 and 6.

The boundary of the bearing failure at each bolt was measured accurately and the bearing failure envelope passing through these boundary points (mean values of the measured coordinates) was plotted for each bolt as shown in Fig. 16 and 17. It is observed from these plots that even though the specimens are cut from a quasi-isotropic laminate with symmetric ply layup, loaded symmetrically in the INSTRON universal testing machine, all the plots are not symmetric. Same observation is applicable to other specimens also. It is observed that the ordinates of the bearing failure boundary is more for the bolt 1 and bolt 2 than bolts 3 and bolt 4. This indicates that the row of bolts close to the free edge of the specimen carries relatively more load than the inner bolts. This observation is in agreement with the results shown by Yang et al. (1998).

From Fig. 18, for specimens T3D6E3W6 - 1 to 5, it is observed that the bearing failure boundary points have a closely resembling spread for Hole – 1 & Hole – 2 and Hole – 3 & Hole – 4. It is noted that the maximum ordinate of the bearing failure boundary on Hole -1 and Hole 2 is higher than the ordinates of the bearing failure boundary on Hole -3 and Hole 4. This indicates that bearing stress at Hole – 1 and Hole – 2 is higher than the bearing stress at Hole – 3 and Hole – 4. This indicates that the failure of the specimen will be initiated around Hole – 1 and Hole – 2. However, the results of the tests have shown the failures both on the load and grip side (Fig. 9). Similar observations are applicable for the specimens T4D6E3W6 - 1 to 5 (Fig. 11) and T5D6E3W6 - 1 to 5 (Fig. 12). The bearing failure envelope passing through the measured boundary points of bearing failure zone was compared with the characteristic curves proposed in the literature (Libin et al., 2015) as shown in Fig. 18. It is observed that the characteristic length in tension proposed is more than that measured from the failed specimens, while, characteristic length in compression proposed is less than that measured from the failed specimens (Fig. 18).

Table 10
Failure load recorded for T3D6E3W6 specimens.

Specimen ID	Thickness (mm)	F_{max} , N	Mean (N)	Standard Deviation (N)	Coefficient of Variation (%)
T3D6E3W6-1	3.328	55673.58	57820.11	1943.33	3.36
T3D6E3W6-2	3.328	59457.96			
T3D6E3W6-3	3.328	55841.28			
T3D6E3W6-4	3.328	59698.85			
T3D6E3W6-5	3.328	58428.89			

Table 11
Failure load recorded for T4D6E3W6 specimens.

Specimen ID	Thickness (mm)	F_{max} , N	Mean (N)	Standard Deviation (N)	Coefficient of Variation (%)
T4D6E3W6-1	4.502	71144.44	73549.13	1780.12	2.42
T4D6E3W6-2	4.502	74823.97			
T4D6E3W6-3	4.502	75720.29			
T4D6E3W6-4	4.502	73104.08			
T4D6E3W6-5	4.502	72952.87			

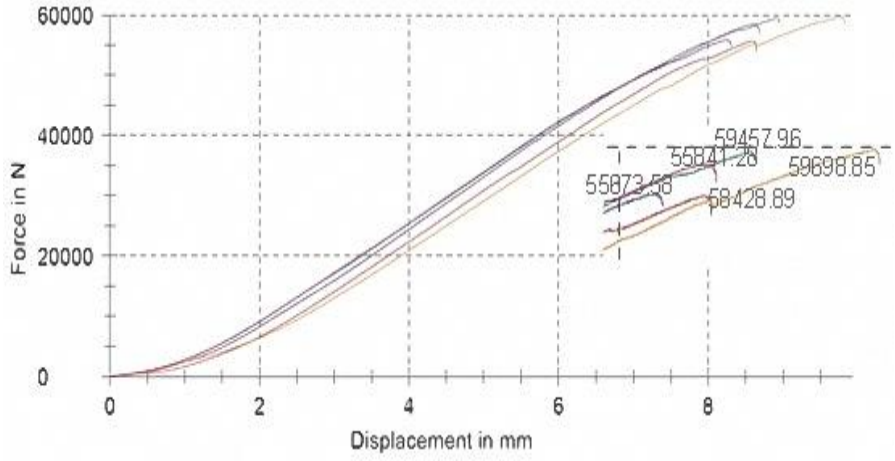

Fig. 13. Load crosshead displacement plot for 3.328 mm thick specimens.

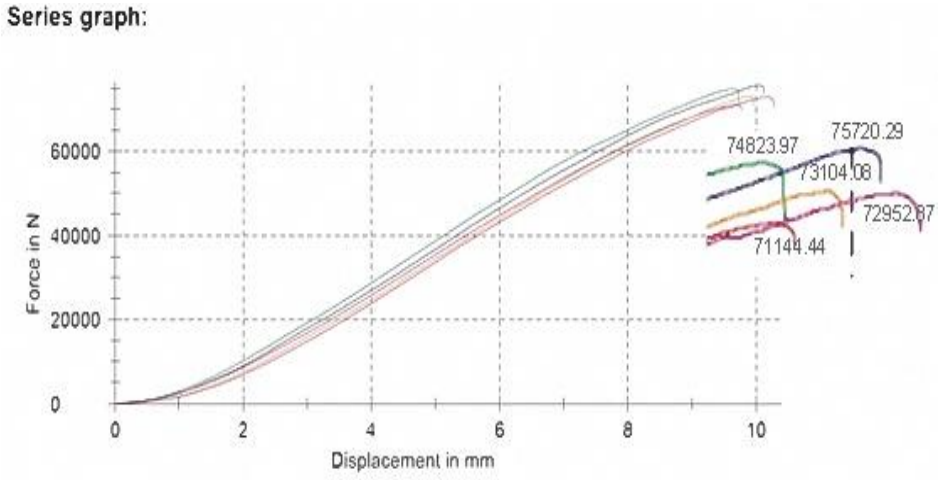

Fig. 14. Load crosshead displacement plot for 4.504 mm thick specimens.

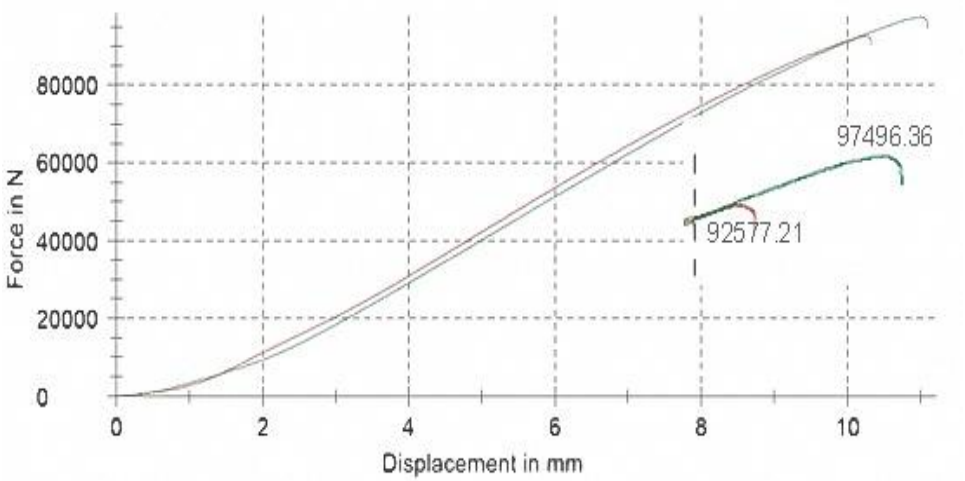

Fig. 15. Load crosshead displacement plot for 5.665 mm thick specimens.

Table 12
Failure load recorded for T5D6E3W6 specimens.

Specimen ID	Thickness (mm)	F_{max} , N	Mean (N)	Standard Deviation (N)	Coefficient of Variation (%)
T5D6E3W6-1	5.672	NA	95036.84	3478.29	3.66
T5D6E3W6-2	5.672	NA			
T5D6E3W6-3	5.672	NA			
T5D6E3W6-4	5.672	92577.31			
T5D6E3W6-5	5.672	97496.36			

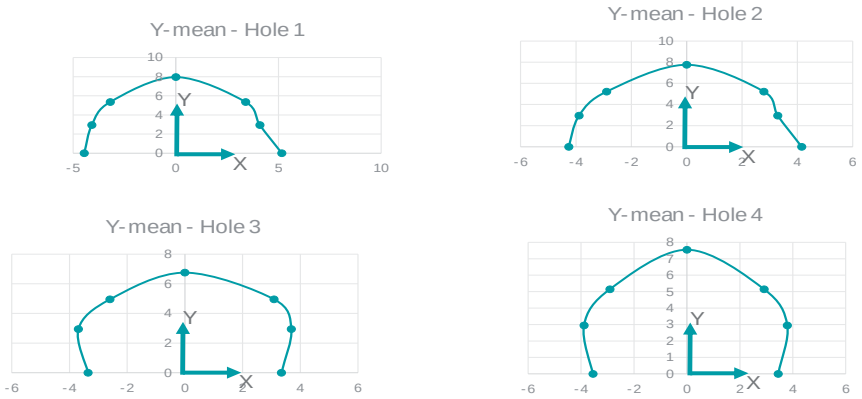

Fig. 16. Boundary of the bearing failure zone for specimens T3D6E3W6-1 to 5.

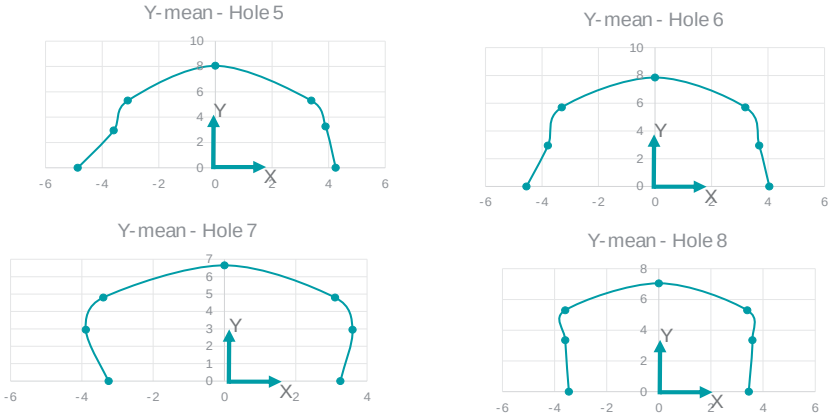

Fig. 17. Boundary of the bearing failure zone for specimens T3D6E3W6-1 to 5.

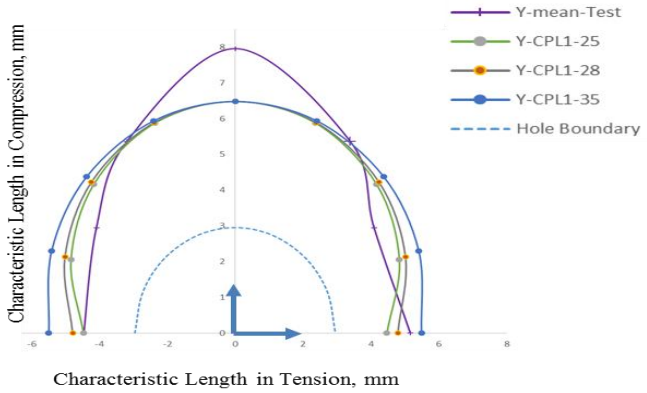

Fig. 18. Mean test bearing failure - proposed characteristic curves in literature – Hole 1 T3D6E3W6.

6.2. Numerical results

The numerical analysis was carried out using ANSYS code. Three finite element models were used to study the behavior of the specimens. The analysis is carried out in two load steps. In the first load step, only bolt preload is applied; in the second load step the full load is applied in 20 sub steps. With each load increment in sub step, the displacement increased linearly. The finite element plot of the specimen and hole deformations for the three models is shown in Fig. 19 to 20.

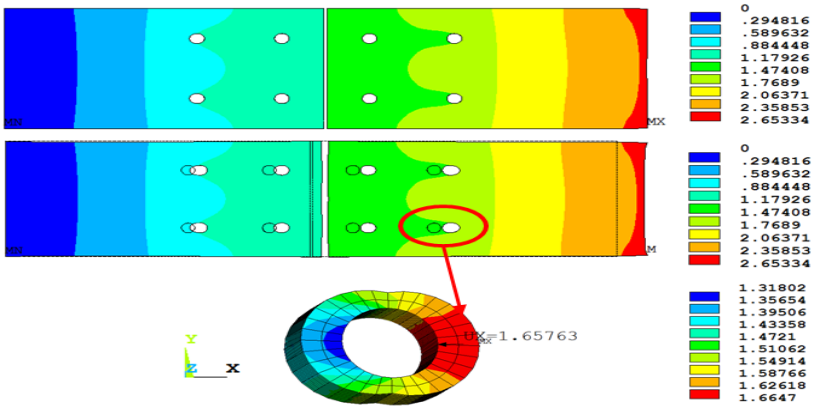

Fig. 19. Specimen and bolt hole deformation for 3.328 mm thick specimen.

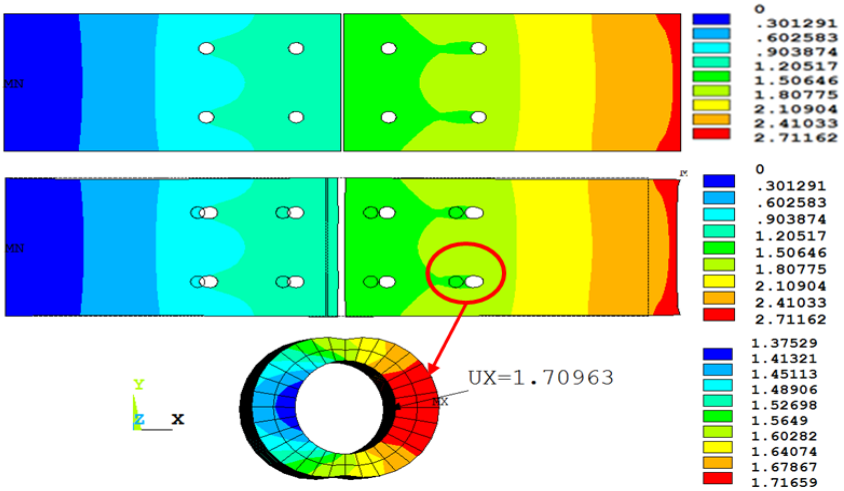

Fig. 20. Specimen and bolt hole deformation for 4.502 mm thick specimen.

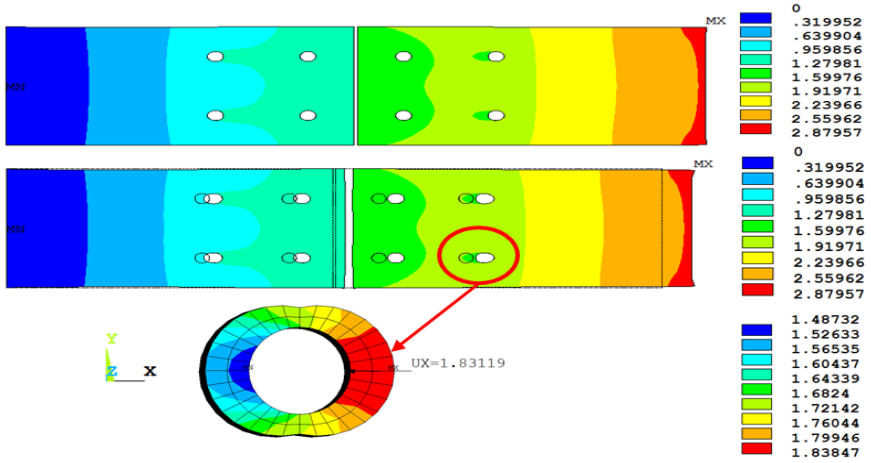

Fig. 21. Specimen and bolt hole deformation for 5.664 mm thick specimen.

6.3. Comparison

As mentioned earlier, Table 6 shows the comparison deformation of the specimen and the deformation of the hole obtained from experimental and numerical studies. It is observed that the variation between the experimental and numerical value of hole deformation varies from as low as 1.20% to as high as 31.46% for the specimens failed on the right grip side, whereas for the specimens failed on the left grip side the variation is between 5.71% to 39%. Similarly, the difference between the experimental and numerical specimen deformation, varies from as low as 1.45% to as high as 21.52% for the specimens failed on the right grip side, whereas, for the specimens failed on the left grip side the variation is between 1.45% and 35.01%. It is observed that the percentage variation in deformation is lowest for specimen of lowest thickness and it increases as the thickness of specimen increases.

7. Conclusion

Results are presented for the 3 sets of specimens of eight bolted joint fabricated using glass Prepreg fabric with quasi-isotropic, symmetric layup. The specimens exhibited bearing failure at all eight bolts followed by net tension failure on both grip side and load side cross sections. The failure load varied from 5 to 6% among the specimens in each set and is an indicator of good fabrication and specimen preparation process. The measured deformation of bolt hole and specimens are found to agree close to the predicted numerical results for thin T3D6E3W6 specimens as compared with T4D6E3W6 and T5D6E3W6. The present study indicates that there are differences in the ordinates between the bearing failure boundary modeled by the incorporated characteristic curve and the measured values from the specimen after the test. This study indicates that the characteristic length in tension is less than and characteristic length in compression as compared to those cited in the literature. The present study indicates that for this type of joint increase in the coefficient of friction between the bolt shank and laminate doesn't significantly change the deformation of the bolt hole and specimen.

Acknowledgements

The authors gratefully acknowledge the support received by Rajendra Kumar Patro, VP, Cyient limited, for his permission to avail the computational facility and publication of this work at Cyient Limited, Hyderabad. Authors acknowledge gratefully the support by Mr. Srinivasa Rao and his team of Allen Reinforced Plastics (P) limited in the fabrication and preparation of specimens. The testing support provided by the Dr. Ramesh Sundaram and team of Advanced Composite Division of National Aerospace Laboratories, Bangalore is acknowledged with due sincerity.

This research did not receive any specific grant from funding agencies in the public, commercial, or not-for-profit sectors. The Authors declare that there is no conflict of interest. We have also attached the signed forms to this effect.

References

Abid, M., Mehmood Khan, Y., 2013. The effect of bolt tightening methods and sequence on the performance of gasketed bolted flange joint assembly. Struct. Eng. Mech., 46(6), 843-852.

ASTM D 5961 / D 5961M-08, 2010. Standard test method for bearing response of polymer matrix composite laminates.

Binqi, C., Mingbo, T., Yiding, W., Fangli, W., 2015. Numerical analysis of composite bolted joints using the Arlequin method. 3rd International Conference on Material, Mechanical and Manufacturing Engineering (IC3ME 2015), 2051-2055.

Camanho, P.P., Matthews, F.L., 1997. Stress analysis and strength prediction of mechanically fastened joints in FRP: A review, Composites Part A 28A, Elsevier Science Limited, 529-547.

Gray, P.J., McCarthy, C.T., 2010. A global bolted joint model for finite element analysis of load distributions in multi-bolt composite joints. Science Direct, Composites Part B: Engineering, 41(4), 317-325.

Hilton, A., 2016. Bearing stresses in bolted composite joints with different contact interactions. Int. J. Eng. Technol., 8(2), Apr-May.

Ivana, I., Zlatko, P., Mirko, M., Slobodon, S., Dragi, S., 2011. Computation method in failure analysis of mechanically fastened joints at layered composites. J. Mech. Eng., 553-559.

Jean-Michel, M., 2016. Optimal tightening process of bolted joints. Int. J. Simulat. Multidiscipl. Des. Optim., Monville, J.M., Published by EDP Sciences.

Katsumata, T., Mizutani, Y., Todoroki, A., Matsuzaki, R., 2010. A study on failure behavior of CFRP bolted joints with cone washers by using AE monitoring. EWGAE 2010 8 -10 September, NDT net.

Khurshid, H., 2013. Effect of bolt layout on the mechanical behavior of four bolted shear joint using three-dimensional finite element analysis. J. Mech. Eng. Technol., 5(2), 119-136.

Kunliang, L., Ying, T., Cheng, L., 2013. Effects of pre-tightening force and connection mode on the strength and progressive damage of composite laminates with bolted joint. Mater. Phys. Mech., 18(2013), 18-27.

Libin, Z., Tianliang, Q., Jianua, Z., Yuli, C., 2015. 3D gradual material degradation model for progressive damage analysis of unidirectional composite materials. Mathematical problems in engineering, 145629, 11.

Longquan, L., Ying, M., Ran, W., 2011. An analytical tool to predict load distribution of multi-bolt single lap thick laminate joints. ICCM18, ICC Jeju, Korea August 21-26.

McCarthy, C.T., McCarthy, M.A., 2005. Three-dimensional finite element analysis of single-bolt, single-lap composite bolted joints: Part II – effects of bolt-hole clearance. Compos. Struct., 71, 159-175.

McCarthy, C.T., McCarthy, M.A., Stanley, W.F., 2005. Experiences with modeling friction in composite bolted joints. J. Compos. Mater., 39, 1881-1908.

McCarthy, M.A., Lawlor, V.P., Stanley, W.F., 2002. Bolt-hole clearance effects and strength criteria in single-bolt, single-lap, composite bolted joints. Compos. Sci. Technol., 62, 1415-1431.

McCarthy, M.A., McCarthy, C.T., 2013. Finite element analysis of the effects of clearance on single shear, composite bolted joints. The Institute of Materials, London, UK. J. Plast. Rubber Compos., 32(2).

McCarthy, M.A., McCarthy, C.T., Lawlor, V.P., 2005. Three-dimensional finite element analysis of single-bolt, single-lap composite bolted joints: Part I – model development and validation. Compos. Struct., 71, 140-158.

Metallic Materials Properties Development and Standardization, MMPDS-07, April 2012.

Michelle, M., Yeow, N., Ed Hooper, 2013. Advanced composites group, ACG MTM45-1 6781 S-2 glass 35% RC qualification material property data report, SP3505WI-Q. National Institute of Aviation Research (NIAR).

Nasraoui, M.T., Chakhari, J., Khalfi, B., Nasri, M., 2013. Numerical and experimental study of shear loaded bolted joint. Int. J. Curr. Eng. Technol., INPRESSCO, 239-243.

Olanrewaju, A., 2011. An analytical method for failure prediction of composite pinned joints. Proceedings of the World Congress on Engineering, Vol III, WCE 2011, July 6 - 8, 2011, London, U.K.

Sen, F., Pakdil, M., Sayman, O., Benli, S., 2007. Experimental failure analysis of mechanically fastened joints with clearance in composite laminates under preload. Science Direct, Materials and Design, 1159-1169.

Shirazi, M.V., Zareb, A., 2013. Investigation of 3-D friction coefficient in pinned composite plates. Sci. J. Pure Appl. Sci., 2(8), 299-313.

Sreeshankar, K.K., Amal Hisham, E., Shereef, A.D., Dhanush, V., 2014. Three dimensional finite element analysis of single bolted Aluminum lap joint and validation by XRD technique. Proceedings of 3rd IRF International Conference, 17-21.

Unbrako Engineering Guide.

Xiao, Y., Wang, W., Takao, Y., Ishikawa, T., 2000. The effective friction coefficient of a laminate composite, and analysis of pin-loaded plates. J. Compos. Mater., 34, 69-87.

Yang, X., Zhang, Y., Xiwu, X., 1998. A strength analysis method for composite plate with multiple bolted joints. Act Aeronautica Et Astronautica Sinica, 1998-01.

How to cite this article: Subramanya Sastry, S.S., Nagaraju Reddy, V.S., Ramjeyathilagam, K., 2017. Experimental and numerical studies of laminated butt joint specimens with Aluminum butt straps under preload. Scientific Journal of Pure and Applied Sciences, 6(9), 635-650.